Case Study: Effect of Suction Valve Control and Timed Coolant Injection on Reciprocating Compressors

A.C. Plekker[a] and G.G. Jacobs[b]

Received 22 February 2025, in revised form 18 February 2026 and accepted 25 August 2026

Abstract: ***Reciprocating compressors have many applications ranging from household to industrial use. These compressors are mostly powered by electricity generated from fossil fuels, which contribute to global warming. The aim of this research was to investigate the effects of timed coolant injection in a reciprocating compressor, creating a quasi-isobaric process followed by a quasi-isothermal process to increase compressor efficiency. Water was used as coolant. A mathematical model, based on the First Law of Thermodynamics, of a reciprocating air compressor with coolant injection and suction-valve control was developed. This model was validated against experimental results, which showed savings in indicated work of 5.7%, 10.8% and 10.3% for pressure ratios of 4, 5.5 and 7, respectively. Simulations, without validation for a pressure ratio of 10, indicated work savings of 9.2 - 9.4%. The model can be used as a design aid for developing future reciprocating compressors with improved efficiency, thereby reducing electricity consumption.***

Additional keywords: Reciprocating compressor; Coolant injection; Suction valve control; Compressor efficiency; Quasi-isothermal; Quasi-isobaric

1 Introduction

Compressed air is used throughout various industries with uses ranging from small pneumatic tools in the manufacturing sector to long pipelines at mines. The wide use of compressed air equates to between 9 and 10% of total electricity consumption in industry worldwide [1]. Compressed air is an inefficient form of energy with only up to 19% of the energy consumed converted into usable work [1, 2, 3]. Thermal energy lost to the surroundings constitutes the largest part of the total energy loss of a compressed air system [2]. The overall efficiency of a compressor is derived from the product of the electrical, mechanical and isentropic efficiency, with the latter also the least efficient at between 80–83% [4]. The overall efficiency of compressors depends on the design, type and size of the compressor but ranges from 65% for rotary screw compressors to 90% for slow-speed reciprocating compressors [1]. An increase in compressor thermal efficiency would thus yield an increase in the overall compressor efficiency and compressed air system efficiency.

Compressor efficiency can be maximised if the working cycle is internally reversible, that is, the working fluid and its surroundings is in a constant state of equilibrium [5, 6]. This can be approximately achieved if the compression and expansion processes occur at a slow rate. This slow rate enables the working fluid to absorb or dissipate heat to achieve energy equilibrium at each time step. In practice, an internal reversible process cannot be achieved within reasonable practical and economical limits. The equilibrium state of an internally reversible compressor can be imitated through various means to achieve a quasi-equilibrium state [7]. This quasi-equilibrium state is achieved through the effective cooling of the working fluid during compression.

The efforts to cool the working fluid during compression can be grouped into two main categories, namely external and internal cooling, as shown in Figure 1. External cooling of compressors is accomplished with external fins on the cylinder, using a cooling fan, cooling jacket, or inter-stage cooling [8, 9]. In-cylinder cooling is accomplished with dry compression methodologies such as utilising a finned cylinder head and piston [10]. Wet compression is achieved with coolant injection or liquid pistons [7, 11, 12]. The majority of research conducted on quasi-isothermal compression encompasses the introduction of liquid coolant into the compression chamber. The coolant can be either mixed with the gas prior to the commencement of the suction stroke or directly injected into the cylinder during compression. This results in direct heat exchange between the compressed gas and coolant, i.e., a directly cooled compression process.

Coolant, in the form of oil, refrigerant or water, is injected directly into the cylinder during the compression stroke [13, 14]. The injected coolant mixes with the working fluid and absorbs the heat generated during compression, resulting in a quasi-isothermal process [7, 15].

Research pertaining to direct water coolant injection to obtain quasi-isothermal compression was performed by Coney et al. [7], which highlighted the factors influencing heat transfer with 3D computational fluid dynamics simulations. Coney et al. stressed that a limited time is available to inject water into the cylinder, but that two approaches can be taken, namely early injection and late injection. Early injection, which occurs during the suction stroke, has the benefit of a high droplet dispersion and penetration rate; however, this results in a low

[a] Department of Mechanical and Mechatronic Engineering, Central University of Technology, Free State, South Africa. E-mail: carelplekker@gmail.com

[b] ORCID 0000-0002-6152-4356. Department of Mechanical and Mechatronic Engineering, Central University of Technology, Free State, South Africa. E-mail: gjacobs@cut.ac.za. (Corresponding author)

http://dx.doi.org/10.69694/2309-8988/2026/v42a3

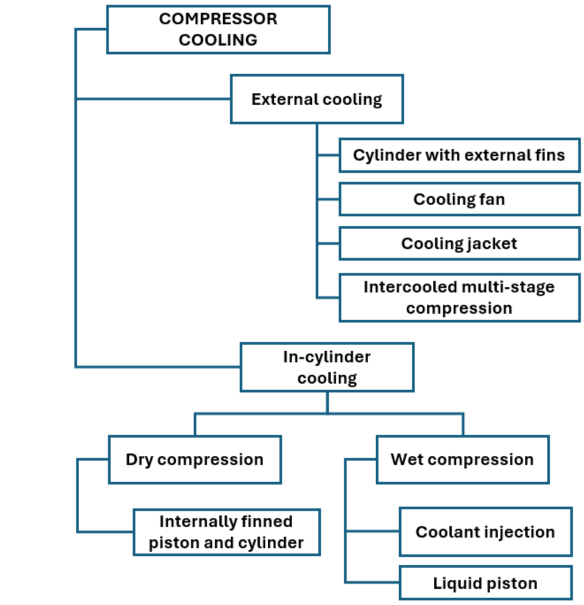

Figure 1 Compressor cooling methods

droplet velocity during the compression stroke, lowering the heat transfer rate at the point of high heat generation. Late injection, which occurs during the compression stroke, is the desired injection period, with heat generation being the highest, but with a higher working fluid density, which results in poor droplet penetration to the centre of the cylinder. This problem was overcome by increasing the size of the water droplets injected into the cylinder during the compression stroke.

Malmgren et al. [16] subsequently created and validated a 1-D dynamic mathematical model to simulate the compressor tested by Coney et al. Jacobs and Liebenberg [15] have shown that even higher compressor efficiencies can be obtained. The process proposed by Jacobs and Liebenberg involved isobaric cooling at the commencement of the compression stroke, through suction valve control, followed by isothermal compression. The process is depicted on T–S and P–V diagrams in Figure 2.

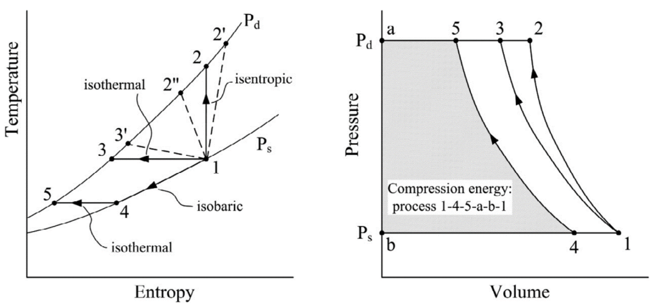

Figure 2 Temperature–entropy and pressure–volume diagrams showing energy saving if isobaric compression is followed by isothermal compression.

The isobaric cooling process (process 1–4 in Figure 2) is achieved by a sudden and significant cooling effort, achieved with water coolant injection, at the commencement of the compression stroke. The authors found that the increase in density of the working fluid, due to the coolant injection, created a quasi-isobaric compression process, which resulted in a decrease in work done during the initiation of the compression stroke.

The quasi-isobaric conditions can only be achieved if the suction valve is kept closed during coolant injection. The authors utilised a camshaft to control the suction valve and actuate the coolant injection valves. A mathematical model was created by Jacobs and Liebenberg to describe this novel compression process [15, 17]. This mathematical model was based on describing the compression and expansion processes as polytropic processes. The authors noted that the limitation to the mathematical model is the polytropic index, which should be determined through experimentation. It was proposed to create a similar model based on the First Law of Thermodynamics to better investigate the effect of timed cooling and to determine the amount of heat removed during isobaric cooling.

2 Methodology

The schematic depicting the compressor model is shown in Figure 3. The working fluid enters the cylinder through the suction valve at a rate of $\dot{m}_s$, temperature T_s and pressure P_s, while leaving through the discharge valve at a rate of $\dot{m}_d$, temperature T_d and pressure P_d. It is assumed that no spatial variation in pressure or temperature is present inside the cylinder, and piston ring leakage and other non-idealities are ignored.

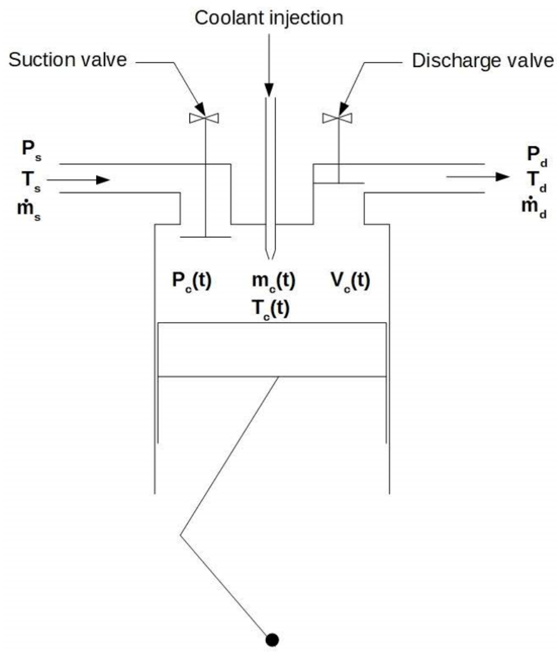

Figure 3 Schematic of compressor model

2.1 First Law of Thermodynamics model

The model created for this study is based on the thermodynamic model used by Singh and Patel [18], which was used to simulate an oil-flooded twin-screw compressor. The First Law of Thermodynamics states that for a closed system undergoing a process, the increase in internal energy (ΔU) equals the work supplied to the system (W) less the heat rejected by the system (Q):

http://dx.doi.org/10.69694/2309-8988/2026/v42a3

$$\Delta U = W - Q \tag{1}$$

Continuity of mass is expressed as:

$$\frac{dm}{dt} = \dot{m}_s - \dot{m}_d \tag{2}$$

where $\frac{dm}{dt}$ is the rate of change of mass of the working fluid inside the cylinder, $\dot{m}_s$ the mass flow rate through the suction valve and $\dot{m}_d$ the mass flow rate through the discharge valve.

It is assumed that the working fluid is an ideal gas, adhering to:

$$PV = mRT \tag{3}$$

where P is the instantaneous pressure, V is cylinder volume, m is the working fluid mass, R is the gas constant and T cylinder gas temperature. The ideal gas assumption is generally valid for reduced pressure $P_r = \frac{P}{P_{critical}} \leq 0.1$ and reduced temperature $T_r = \frac{T}{T_{critical}} \geq 2$ [5]. With the maximum validation case pressure ratio being 7 at testing atmospheric pressure of ≈ 85 kPa *abs*. renders maximum cylinder pressure of ≈ 600 kPa *abs*. Consequently, the ideal gas error is less than 1%. For higher pressures, real gas properties should be used in simulations.

Heat transfer through the cylinder wall can be expressed as:

$$\dot{Q} = h_w A (T_w - T) \tag{4}$$

where h_w is the coefficient of heat transfer of the cylinder wall, A is the total area of the cylinder wall in contact with the working fluid and T_w is the instantaneous cylinder wall temperature.

Differentiating equation (1) and combining equations (1)–(4), noting that $\gamma = \frac{c_p}{c_v}$ and $R = c_p - c_v$ an equation can be derived for the instantaneous cylinder pressure:

$$\frac{dP}{dt} = \frac{R\gamma}{V}(\dot{m}_s T_s - \dot{m}_d T) + \frac{R h_w A_w}{c_v V}(T_w - T) - \frac{dV}{dt}\frac{P}{V}\left(\frac{R}{c_v} + 1\right) \tag{5}$$

2.2 Modelling of cylinder volume rate of change

The compressor was modelled as crank-driven. An equation to describe a crank-driven compressor's cylinder volume at any moment was expressed by Srinivas et al. [19] as:

$$V = V_{cle} + \frac{V_{str}}{2}\left[1 - \cos(\omega t)\right] \tag{6}$$

where V_{cle} is cylinder clearance volume, V_{str} is stroke volume, ω is crank angular velocity and t is time. The solving of equation (5) requires the rate of change in compressor volume, $\frac{dV}{dt}$. This can be found by differentiating equation (6):

$$\frac{dV}{dt} = \frac{V_{str}}{2}\omega \sin(\omega t) \tag{7}$$

2.3 Mass flow through valves

A common approach is to model the flow of the working fluid through the valve as an orifice with an equivalent diameter [15, 19]. The mathematical model followed the approach set forth by Srinivas and Padmanabhan [19], who consider their valve mass flow as flow through an orifice:

$$\dot{m}_s = \begin{cases} C_{D,s}\rho_s A_{sv}\sqrt{\dfrac{2(P_s - P_i)}{\rho_s}}, & P_s > P_i \text{ and } x_s > 0 \\ -C_{D,s}\rho_i A_{sv}\sqrt{\dfrac{2(P_i - P_s)}{\rho_i}}, & P_i > P_s \text{ and } x_s > 0 \end{cases} \tag{8}$$

$$\dot{m}_d = \begin{cases} C_{D,d}\rho_i A_{dv}\sqrt{\dfrac{2(P_i - P_d)}{\rho_i}}, & P_i > P_d \text{ and } x_d > 0 \\ -C_{D,d}\rho_d A_{dv}\sqrt{\dfrac{2(P_d - P_i)}{\rho_d}}, & P_d > P_i \text{ and } x_d > 0 \end{cases} \tag{9}$$

where P_s, P_d and P_i are respectively the suction pressure, discharge pressure and instantaneous in-cylinder pressure; ρ_s, ρ_d and ρ_i are respectively the suction density, discharge density and instantaneous in-cylinder density; $C_{D,s}$ and $C_{D,d}$ are the suction and discharge valve coefficients; A_{sv} and A_{dv} are the suction and discharge valve flow areas; and x_s and x_d are the instantaneous valve displacement heights for the suction and discharge valve plates respectively.

2.4 Modelling valve dynamics

Valves were modelled as spring-mass-damper systems with a single degree of freedom [20, 21, 22, 23] with the following equation:

$$m_v\frac{d^2x}{dt^2} + c\frac{dx}{dt} + \kappa(x + x_{\text{pre}}) = F_{\text{act}} \tag{10}$$

where m_v is the valve plate mass, x is valve displacement, c is the damping coefficient, κ is the spring stiffness, and F_{act} is the valve actuation force. If a valve limiter is present, the valve will bounce when the limiter is reached.

The spring actuation force is determined by:

$$F_{\text{act}} = C_f A_p \Delta P \tag{11}$$

where A_p is the area of the port, ΔP is the change in pressure, and C_f is a force coefficient which is determined empirically or by use of Böswirth's model [24]. The force coefficient can be determined if the valve entrance friction factor is known:

$$C_f = \frac{1}{1 + \xi\left(\dfrac{A_o C_d}{A_p}\right)} \tag{12}$$

where ξ is the valve entrance friction coefficient and A_o is the valve opening area, otherwise $C_f \approx 1$ [24].

2.5 Modelling coolant injection

Heat transfer in the compressor subjected to coolant injection occurs between (a) the working fluid (gas that is being compressed) and the cylinder wall and (b) between the working fluid and the injected coolant. The heat transfer from the working fluid to the cylinder wall is calculated with Eq. (4). If an isothermal or quasi-isothermal compression process is

http://dx.doi.org/10.69694/2309-8988/2026/v42a3

considered, then heat transfer to the cylinder wall will be negligible.

The heat transfer from the working fluid to the injected coolant is assumed to be an adiabatic mixing process. An adiabatic mixing process was selected since the heat transfer from the cylinder to its surroundings is negligible and the in-cylinder mixing process involves no work [5]. For adiabatic mixing, the energy balance becomes:

$$\dot{m}_s h_s + \dot{m}_c h_c = \dot{m}_d h_d \tag{13}$$

where $\dot{m}_c$ is the coolant mass flow, and h_s, h_c and h_d are the suction, coolant and discharge specific enthalpies, respectively. For an ideal gas, the specific enthalpy can also be written as $h = c_p T$, thus reducing Eq. (13) to:

$$\dot{m}_s c_{p_s} T_s + \dot{m}_c c_{p_c} T_c = T_d \sum (\dot{m} c_p) \tag{14}$$

2.6 Solution algorithm

Equations (5), (7), and (10) are first- and second-order nonlinear ordinary differential equations (ODEs). This system of differential equations must be solved simultaneously to simulate the workings of the compressor.

The fourth-order Runge-Kutta method was chosen to solve these equations for its ease of implementation. The formula to solve ODEs with the fourth-order Runge-Kutta method is:

$$\begin{aligned}
K_1 &= f(t_i, y_i) \\
K_2 &= f\left(t_i + \frac{\Delta t}{2}, y_i + \frac{\Delta t}{2} K_1\right) \\
K_3 &= f\left(t_i + \frac{\Delta t}{2}, y_i + \frac{\Delta t}{2} K_2\right) \\
K_4 &= f(t_i + \Delta t, y_i + \Delta t K_3) \\
y_{i+1} &= y_i + \frac{\Delta t}{6}(K_1 + 2K_2 + 2K_3 + K_4)
\end{aligned} \tag{15}$$

where t is time, subscript i is the time step, Δt is the time step size and y is the variable to be solved. The Runge-Kutta method can be used to solve multiple ODEs simultaneously by adding the variables to the function.

3 Experimental results used for model validation

The experimental results of Jacobs [17] were used for validation of the mathematical model presented in this article. Descriptions of the experimental setup, measurement uncertainties, experimental procedure and experimental data reduction are described in [15] and [17]. To ensure that the suction valve stayed closed during coolant injection, the experimental compressor was equipped with a cam-actuated suction valve. Coolant injector actuation was also accomplished through cam actuation. The coolant was water. To inhibit corrosion, an additive for water hydraulics, Hydrocool 120 from the Petrofer company, was added at 5% volume ratio.

4 Results and discussion

Jacobs [17] utilised functional analysis to quantify the difference between the experimental and modelled data. The Euclidean Relative Difference (ERD), Euclidean Projection Coefficient (EPC) and Secant Cosine (SC) were used. The ERD evaluates the average difference between the experimental and model data; thus, an ERD value of zero would suggest a perfect curve fit. The EPC is a factor which would provide a perfect curve fit between the modelled and experimental data when multiplied by the experimental data. An EPC of one would imply a perfect curve fit. SC evaluates the fit of the modelled data curve according to its shape relative to the shape of the experimental data curve. A perfect shape fit would render an SC of one.

The acceptance tolerance limit used during validation was 20%, meaning that the modelled data is not to deviate further than ERD ≤ 0.2, $0.8 \leq$ EPC ≤ 1.2 and SC ≥ 0.8. The validation statistics of all tests fell within the acceptance limits with maximum deviations being 0.141, 1.118 and 0.952 for the ERD, EPC and SC values respectively. The average validation statistics for all test groups are tabulated in Table 1.

Table 1 Validation statistics.

Test group	ERD	EPC	SC
4 Dry	0.124	0.974	0.952
4 Timed coolant injection	0.139	1.080	0.969
5.5 Dry	0.101	1.054	0.976
5.5 Timed coolant injection	0.141	1.102	0.985
7 Dry	0.133	1.118	0.984
7 Timed coolant injection	0.131	1.107	0.989
Maximum deviation	0.141	1.118	0.952
Average deviation	0.128	1.073	0.976
Minimum deviation	0.086	0.993	0.989

Table 2 Indicated work done per cycle results.

Test group	Average experimental indicated work/cycle (J)	Simulated indicated work/cycle (J)	Error (%)
4 Dry	29.48	31.33	6.3
4 Timed cool. inj.	27.38	29.53	7.9
5.5 Dry	32.23	36.07	11.9
5.5 Timed cool. inj.	26.31	32.17	22.3
7 Dry	33.71	37.53	11.3
7 Timed cool. inj.	32.03	33.65	5.1

Figures 4–9 show representative validation cases for dry compression and compression with timed coolant injection.

The pressure ratio 4 and 7 test groups show good agreement with experimental results with the 5.5 pressure ratio test group showing the largest disparity. It can be seen from Table 2 that when a comparison between the Dry simulated and Timed simulated cases are made, the Timed simulated case indicates a reduction in work per cycle. This reduction in work signifies the advantage gained when employing suction valve control with timed coolant injection in reciprocating compressors.

Table 3 shows the reduction in simulated indicated work

http://dx.doi.org/10.69694/2309-8988/2026/v42a3

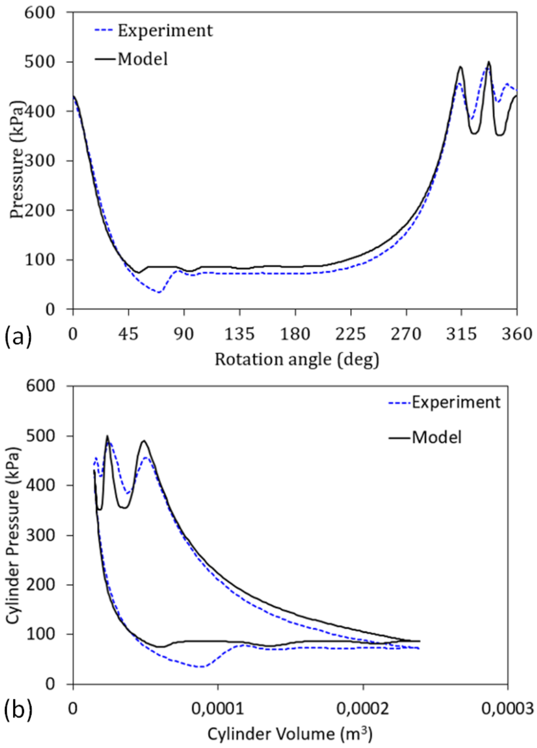

Figure 4 Validation case: Dry compression (Case 4): Experimental vs. modelled results. Cylinder pressure vs. rotation angle (a), and cylinder pressure vs. cylinder volume (b).

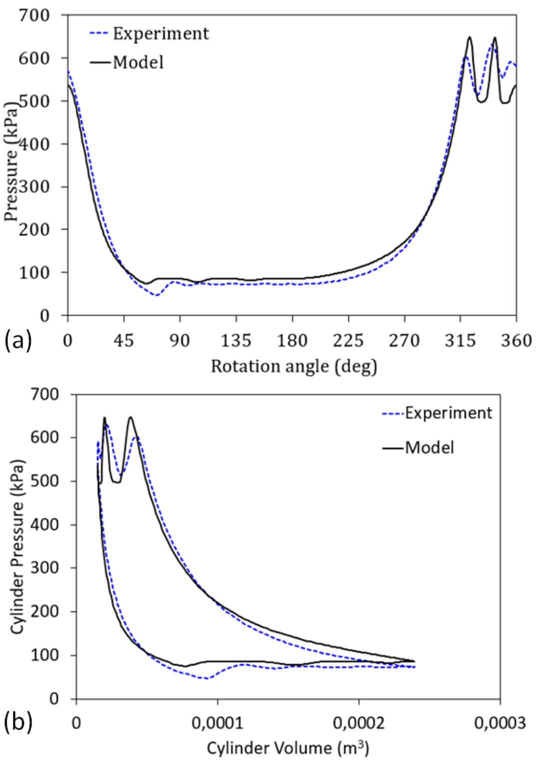

Figure 5 Validation case: Dry compression (Case 5.5). Experimental vs. modelled results. Cylinder pressure vs. rotation angle (a), and cylinder pressure vs. cylinder volume (b).

per cycle for each test group in Joule and as a percentage. It can be seen that the effect of the timed coolant injection with

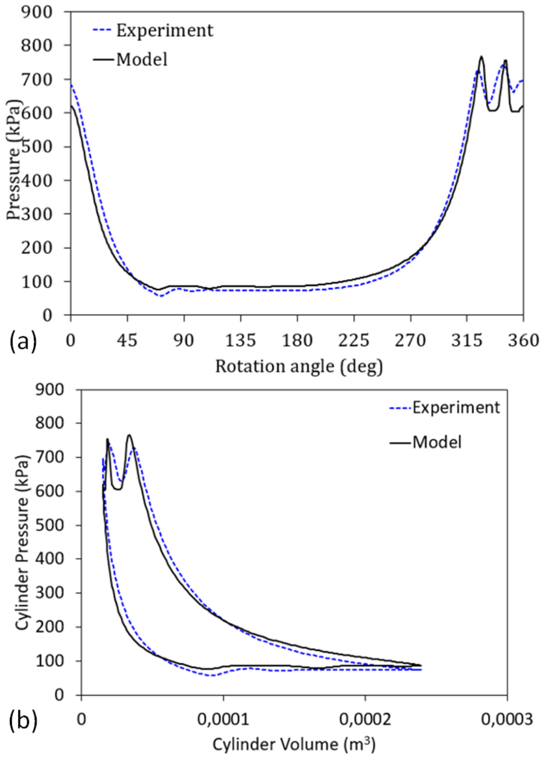

Figure 6 Validation case: Dry compression (Case 7). Experimental vs. modelled results. Cylinder pressure vs. rotation angle (a), and cylinder pressure vs. cylinder volume (b).

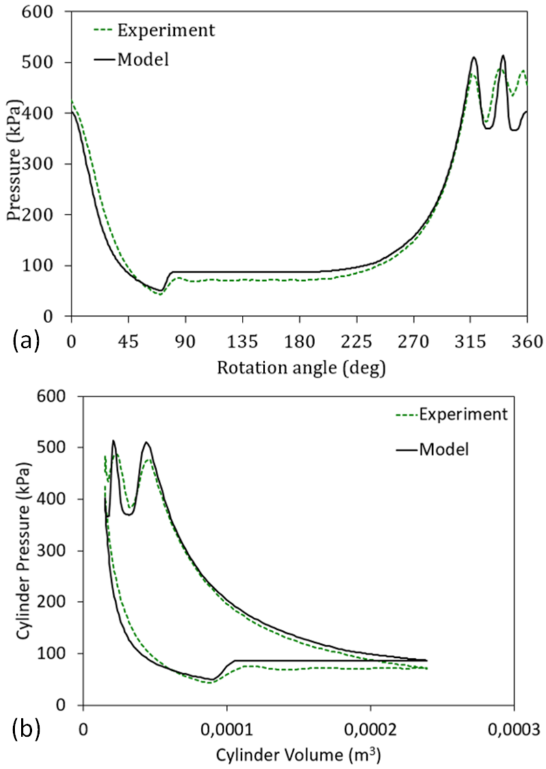

Figure 7 Validation case: Compression with timed coolant injection (Case 4 Timed). Experimental vs. modelled results. Cylinder pressure vs. rotation angle (a), and cylinder pressure vs. cylinder volume (b).

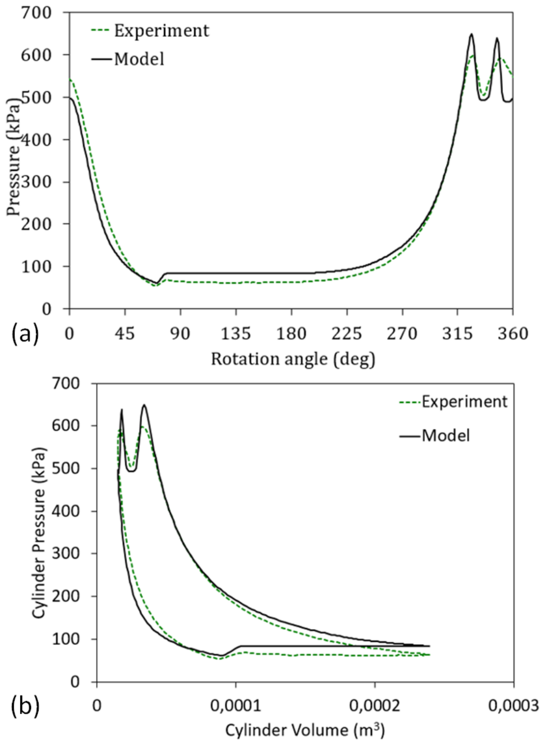

Figure 8 Validation case: Compression with timed coolant injection (Case 5.5 Timed). Experimental vs. modelled results. Cylinder pressure vs. rotation angle (a), and cylinder pressure vs. cylinder volume (b).

suction valve control increases as the pressure ratio increases, Figure 10 . Therefore, an investigation into the application of the model beyond its tested range with a higher pressure ratio was conducted, Figures 11–13.

Table 3 Simulated effect of timed coolant injection with suction valve control for all test groups.

Test group	Simulated indicated work/cycle (J)	Reduction in simulated indicated work/cycle (J)	Energy saving (%)
4 Dry	31.33	–	–
4 Timed cool. inj.	29.53	1.8	5.7
5.5 Dry	36.07	–	–
5.5 Timed cool. inj.	32.17	3.9	10.8
7 Dry	37.53	–	–
7 Timed cool. inj.	33.65	3.9	10.3
10 Dry	31.85	–	–
10 Timed	28.92	2.93	9.2
10 Timed			
-Low T_{coolant}	28.91	2.94	9.2
-MMF	28.86	2.99	9.4

The simulation groups consisted of a Dry and Timed case that was modified to represent the new pressure ratio. Additionally, a simulation case where the injected coolant temperature was decreased to 1 °C (10 Timed-Low T_{coolant}) and a case where the coolant mass flow rate was increased threefold

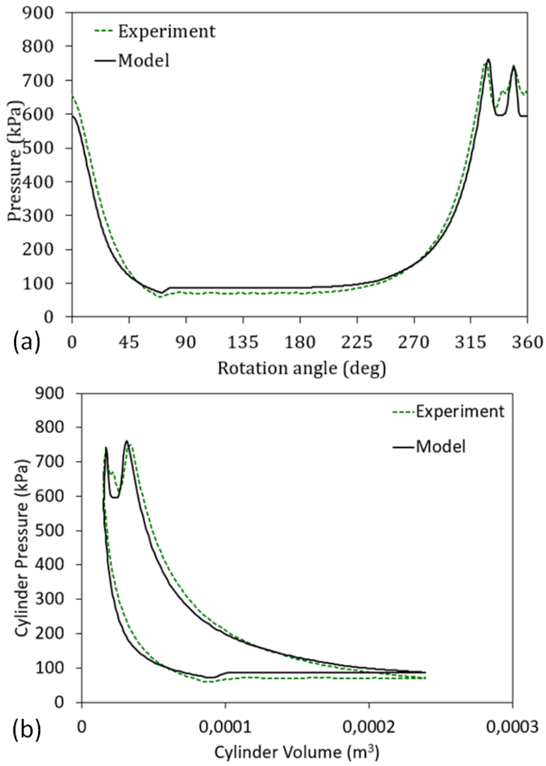

Figure 9 Validation case: Compression with timed coolant injection (Case 7 Timed). Experimental vs. modelled results. Cylinder pressure vs. rotation angle (a), and cylinder pressure vs. cylinder volume (b).

(10 Timed-MMF) was also added. The indicated work per cycle for the Timed-Low T_{coolant} simulated case is similar to the Timed simulation case. However, the indicated work per cycle for the Timed-MMF simulated case was 0.2% less when compared to the Timed and Timed-Low T_{coolant} cases.

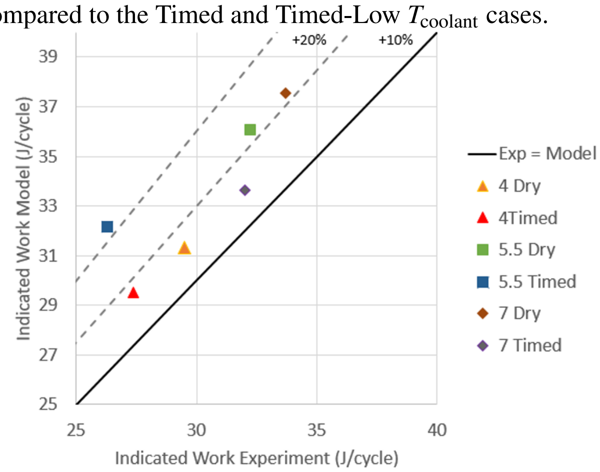

Figure 10 Indicated work per cycle experimental vs. modelled results for all cases.

The percentage of work saved increases from 5.7% for the 4 pressure ratio case to 10.3% for the 7 Timed case. However, the percentage of work saved starts to decrease as the pressure ratio is increased to 10:1. Although the percentage of work saved between the Dry and Timed simulated cases starts to decrease beyond the 5.5 Timed test group, the simulated indicated work per cycle of the Timed simulated cases for the

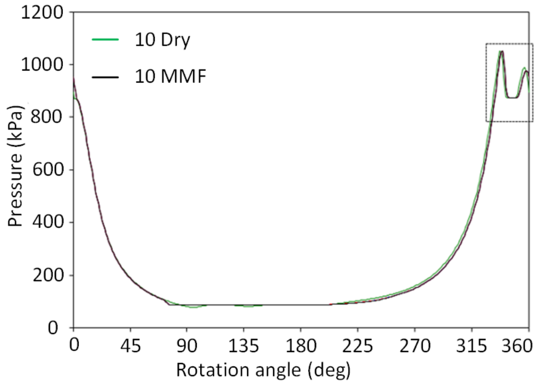

Figure 11 Pressure ratio 10 simulated cases: pressure vs. rotational angle comparison.

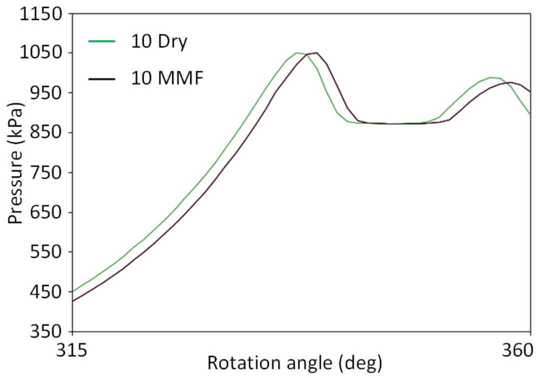

Figure 12 Enlarged area as shown in Figure 11.

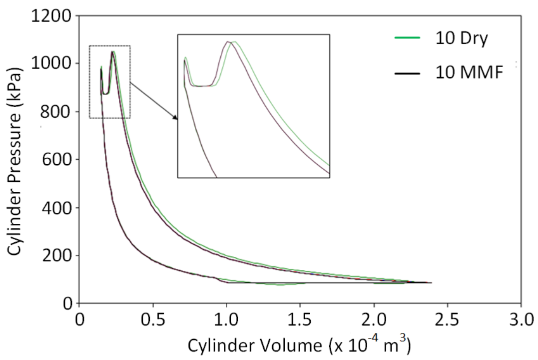

Figure 13 10:1 pressure ratio simulated cases: pressure vs. volume comparison.

10 pressure ratio test group is lower than the 5.5 and 7 Timed cases. This indicates a saving of work per cycle as less work is required to deliver a higher discharge pressure.

5 Conclusion

This research study demonstrated the development and validation of a mathematical model, based on the First Law of Thermodynamics, for a reciprocating compressor subjected to coolant injection and suction valve control. The simulated data were compared with experimental results and showed overall good agreement.

The validated simulation was used to simulate a pressure ratio beyond its tested operating range. The results of this simulation showed that a saving in indicated work can be achieved at higher pressure ratios.

The percentage of work saved increases from 5.7% at a pressure ratio of 4 to 10.3% at a pressure ratio of 7, but begins to decrease as the pressure ratio reaches 10. While the work saved between the Dry and Timed cases drops after the 5.5 Timed group, the simulated work per cycle for the pressure ratio of 10 remains lower than for the 5.5 and 7 Timed cases. This was not expected and should be investigated in future research.

References

[1] R. Saidur, N. A. Rahim, and M. Hasanuzzaman. A review on compressed-air energy use and energy savings. *Renewable and Sustainable Energy Reviews*, 2010. doi: 10.1016/j.rser.2009.11.013.

[2] S. Mousavi, S. Kara, and B. Kornfeld. Energy efficiency of compressed air systems. *Procedia CIRP*, 2014. doi: 10.1016/j.procir.2014.06.026.

[3] J Marais, M Kleingeld, and R Pelzer. Increased energy savings through a compressed air leakage documentation system. *ICUE, SA*, 11:1–6, 2009.

[4] F. A. Ribas, C. J. Deschamps, et al. Thermal analysis of reciprocating compressors - a critical review, 2008. URL `https://docs.lib.purdue.edu/icec/1907`. International Compressor Engineering Conference (Purdue).

[5] Y. A. Cengel and M. A. Boles. *Thermodynamics: An Engineering Approach*. McGraw-Hill, 7 edition, 2011.

[6] T. D. Eastop and A. McConkey. *Applied Thermodynamics for Engineering Technologists*. Pearson Education Limited, 5 edition, 1993.

[7] M. W. Coney, P. Stephenson, A. Malmgren, C. Linnemann, and R. E. Morgan. Development of a reciprocating compressor using water injection to achieve quasi-isothermal compression, 2002. International Compressor Engineering Conference (Purdue).

[8] S. Sun, Y. Zhao, L. Li, and P. Shu. Simulation research on scroll refrigeration compressor with external cooling. *International Journal of Refrigeration*, 33(5):897–906, 2010. doi: 10.1016/j.ijrefrig.2010.03.005.

[9] S. Jarungthammachote. Optimal interstage pressures of multistage compression with intercooling processes. *Thermal Science and Engineering Progress*, 29:101202, 2022. doi: 10.1016/J.TSEP.2022.101202.

[10] M. Heidari, M. Mortazavi, and A. Rufer. Design, modeling and experimental validation of a novel finned reciprocating compressor for isothermal compressed air energy storage applications. *Energy*, 140:1252–1266, 2017. doi: 10.1016/J.ENERGY.2017.09.031.

[11] J. D. Van de Ven and P. Y. Li. Liquid piston gas compression. *Applied Energy*, 86(10):2183–2191, 2009. doi: 10.1016/J.APENERGY.2008.12.001.

[12] C. Qin and E. Loth. Liquid piston compression efficiency with droplet heat transfer. *Applied Energy*, 114: 539–550, 2014. doi: 10.1016/J.APENERGY.2013.10.005.

[13] I. H. Bell, E. A. Groll, and J. E. Braun. Performance of vapor compression systems with compressor oil flooding and regeneration. *International Journal of Refrigeration*, 34(1):225–233, 2011. doi: 10.1016/J.IJREFRIG.2010.09.004.

[14] X. Xu, Y. Hwang, and R. Radermacher. Refrigerant injection for heat pumping/air conditioning systems: Literature review and challenges discussions. *International Journal of Refrigeration*, 34(2):402–415, 2011. doi: 10.1016/J.IJREFRIG.2010.09.015.

[15] G. G. Jacobs and L. Liebenberg. The influence of timed coolant injection on compressor efficiency. *Sustainable Energy Technologies and Assessments*, 18:175–189, 2016. doi: 10.1016/J.SETA.2016.10.010.

[16] M. Malmgren, J. Sidders, P. Stephenson, and M. Coney. Experiments and simulations of a quasi-isothermal compressor for a novel high efficiency engine. In *International Conference on Compressors and their Systems*, pages 461–470, 2003.

[17] G. G. Jacobs. *The influence of controlled coolant injection on quasi-isothermal compression*. PhD thesis, Department of Mechanical Engineering, North-West University, South Africa, 2014.

[18] P. J. Singh and G. C. Patel. A generalized performance computer program for oil flooded twin-screw compressors, 1984. URL `https://docs.lib.purdue.edu/icec`. International Compressor Engineering Conference (Purdue).

[19] M. N. Srinivas and C. Padmanabhan. Computationally efficient model for refrigeration compressor gas dynamics. *International Journal of Refrigeration*, 25(8):1083–1092, 2002. doi: 10.1016/S0140-7007(01)00109-8.

[20] D. Taranović, S. Milojević, and R. Pesić. Modelling valve dynamics and flow in reciprocating compressors, 2013. URL `https://www.researchgate.net/publication/323560736`. Conference paper / technical publication.

[21] R. A. Habing and M. C. A. M. Peters. An experimental method for validating compressor valve vibration theory. *Journal of Fluids and Structures*, 22(5):683–697, 2006. doi: 10.1016/j.jfluidstructs.2006.03.003.

[22] J. Tuhovcak, J. Hejčík, and M. Jícha. Modelling fluid flow in a reciprocating compressor. In *EPJ Web of Conferences*, 2015. doi: 10.1051/epjconf/20159202100.

[23] M. M. Tanveer, C. R. Bradshaw, X. Ding, and D. Ziviani. Mechanistic chamber models: A review of geometry, mass flow, valve, and heat transfer sub-models. *International Journal of Refrigeration*, 142:111–126, 2022. doi: 10.1016/j.ijrefrig.2022.06.016.

[24] L. Boswirth. Non steady flow in valves, 1990. URL `http://docs.lib.purdue.edu/icec/759`. International Compressor Engineering Conference (Purdue).